Diffusion-limited aggregation-like structure induced in Co thin films by carbon ion implantation

1991 J. Phys.: Condens. Matter 3 9551

(http://iopscience.iop.org/0953-8984/3/47/027)

J. Phys.: Condens. Matter 3 (1991) 9551–9557. Printed in the UK

LETTER TO THE EDITOR

Diffusion-limited aggregation-like structure induced in Co thin films by carbon ion implantation

B X Liu†, J Wang‡ and Z Z Fang§

† Centre of Condensed Matter and Radiation Physics CCAST (World Laboratory), Beijing, and Department of Materials Science and Engineering, Tsinghua University, Beijing 100084, People's Republic of China

‡ Department of Materials Physics, University of Science in Technology in Beijing, and Department of Materials Science and Engineering, Tsinghua University, Beijing 100084, People's Republic of China

§ Beijing Institute of Space Physics, Chinese Academy of Science, Beijing 100080, and Department of Materials Physics, University of Science and Technology in Beijing, Beijing 100084, People's Republic of China

Received 4 June 1991

Abstract. Fractal structure of a diffusion-limited aggregation (DLA) type was observed in a Co thin film after 50 keV carbon ion implantation to a dose of 2.5×10^{17} cm^{-2} at room temperature. Our simulation showed that the structure and the aggregating process could be well described within the framework of the DLA model with the following observations. The atoms in the matrix not only play the role of randomizing the track of mobile particles but also take part in the aggregation. The number of steps each particle undergoes is very limited whether it contacts the aggregate or not. Moreover, the particles may be randomly launched anywhere. The correlation dimension of the structure was determined to be about 1.82 ± 0.01.

In recent years, the scientific community has witnessed great advances in the statistical physics of aggregation processes taking place in various random systems, such as dielectric breakdown [1], electro-deposition and sputtered deposition [2], two-fluid displacement in Hell–Shaw cells or fluid displacement in porous media [3], solidification [4], and colloids [5] etc. The work was pioneered by Witten and Sander [6] in the discovery of a diffusion-limited aggregation (DLA) model which leads to various novel patterns and an interesting scaling property. The model has since been extended by modifying some rules in the simulations to recognize various specific essential elements under special conditions, see, for example, the works by Voss [7], Vicsek [8], Botet and Jullien [9] and Meakin and Kobl *et al* [10].

Ion-beam processing was one of the rapidly progressing techniques in the last decade. The basic knowledge of the progress of the projectile ion in a random target is well described by the transport of ions in matter (TRIM) code [11]. Until now, phenomena such as the formation of metastable phases (especially the amorphous phase), ion sputtering, ion-enhanced diffusion, and ion-induced segregation etc, have been studied extensively [12, 13]. Additionally, interesting patterns have recently been observed in

0953-8984/91/479551 + 07 $03.50

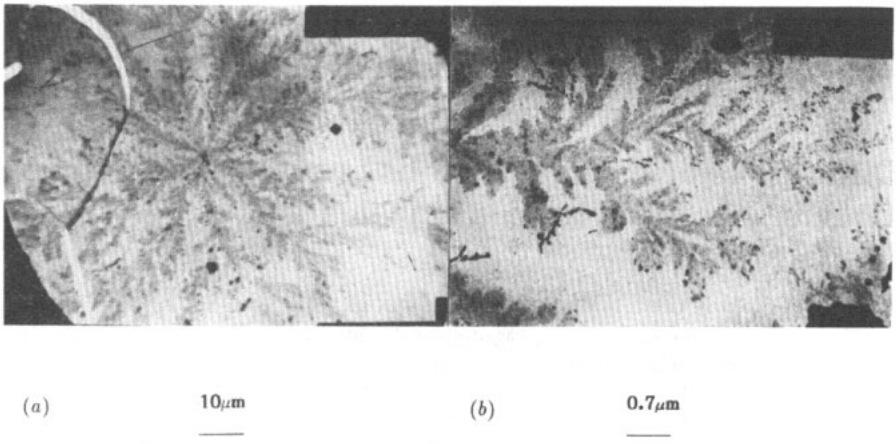

Figure 1. (*a*) A typical dendrite formed on the carbon ion implanted Co thin film at a dose of 2.5×10^{17} cm^{-2} (the film fracture was produced when pressed in between two copper grids on the TEM platform and it is not essential to the explanation). The magnification was $\times 10^3$. (*b*) One enlarged branch of a dendrite, showing the dilation symmetry. The magnification was 1.4×10^4.

our ion-implantation studies [14, 15]. In this letter, we report the observation of DLA-like structures in carbon ion implanted Co thin films, as well as computer modelling to aid the understanding of the structure formed.

The experimental procedures were as follows. Pure metal thin films were deposited onto freshly cleaved NaCl single-crytal substrates in an electron-gun evaporation system with a vacuum of about 2×10^{-6} Torr. The thickness of the films was about 100 nm which was designed by TRIM 88 to match the 50 keV carbon ion range plus longitudinal straggling. The as-deposited films were then implanted at room temperature. To minimize heating by ion implantation the target was water cooled and the ion-beam current density was kept below 1 μA cm^{-2}. After dissolving the NaCl in deionized water, the implanted films were analysed in a JEOL 100CX transmission electron microscope (TEM). A Perkin–Elmer scanning Auger electron microscope (AES) was also employed to confirm the composition.

Figure 1(*a*) shows a typical dendritic structure observed in a carbon ion implanted Co film at a dose of 2.5×10^{17} cm^{-2}. The size of the pattern is about 100 μm as determined from the TEM magnification. Selected-area diffraction on the structure and the matrix showed the same constitution of hexagonal cobalt carbide, as shown in figure 2. High-magnification microscopy did not display any microstructure distinct from the matrix where fine polycrytals were uniformly distributed with a typical size in the ion-induced phase of around 20 nm. From the AES carbon KLL lineshapes at around 272 eV, as shown in figure 3, it was possible to decompose the phase composition of carbon as well as the elemental composition [16]. Because only the hexagonal crystalline phase was observed in TEM, the states of Co could also be estimated from the carbide stoichiometry and the peak-to-peak heights considering the sensitivity factors of different elements in the AES. We obtained the results that approximately 25% of the C is in carbide bonding and 75% is in the amorphous state, while about 40% of the Co is in the carbide and 60% in the amorphous state. The aggregate was therefore situated in a matrix of, and itself was composed of, an amorphous plus carbide polycrystalline phase.

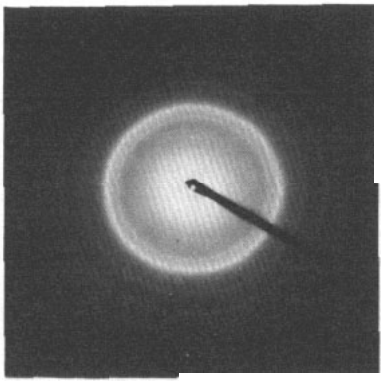

Figure 2. The electron diffraction pattern of hexagonal cobalt carbide.

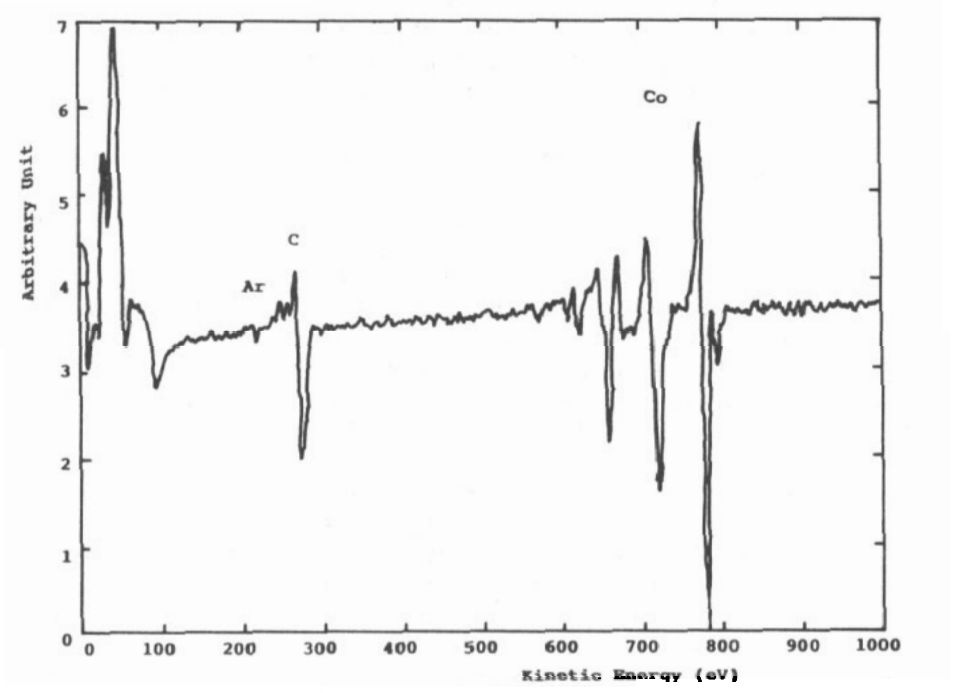

Figure 3. A typical Auger electron spectrum of the films.

The similarity of the structure with that of DLA leads us to study the process in the same manner as DLA. In the DLA model, a seed particle is placed at the origin. Then a mobile particle is released from afar, performs a random walk, terminates when it reaches a site adjacent to the seed and sticks to it. Then another particle is launched in the same way and stops when it contacts the aggregate, and so forth. However, in an ion-beam process, the implanted energetic carbon ions travel in the random (preferably amorphous) solid matrix in a similar zigzag fashion caused by constant collisions—this is simulated by a Markovine random walk. Besides, the recoiled matrix atoms must also

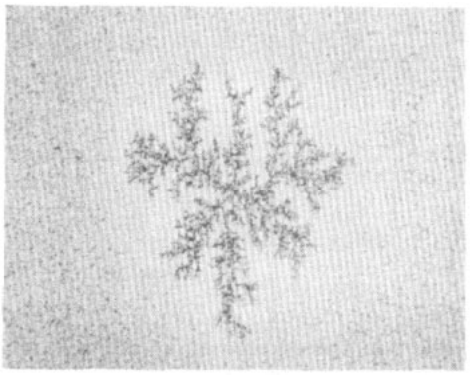

Figure 4. The computer simulation with the limited number of steps and non-restricted launching place modification to the DLA model in a lattice initially distributed with a certain fraction of particles. The fraction was 0.25.

take part in the aggregation. Furthermore, the cohesion among atoms (e.g. the ferromagnetic exchange interaction among Co atoms at a broad range of distances according to the Bethe curve [17]), the long range van der Waals force constantly present among atoms, and clusters of atoms, etc, provides a means for the physical realization of the sticking concept in the DLA model.

However, there are some essential points unique to the ion-beam process. Firstly, it has been estimated that an atom makes about 10–100 jumps and moves a distance of 1–3 nm during the relaxation period [18]. The number of steps in the case of ion irradiation is therefore quite limited, while in the DLA model it is not restricted before the particle terminates on the aggregate or the killing circle designed to reduce unnecessary computer time. Secondly, the particles in the case of ion irradiation may be randomly launched at any place, while in the DLA they are triggered at a distance from the aggregate. Thirdly, the particles initially present in the random matrix must also take part in the aggregation in addition to the implanting particles. The effect of these modifications to the DLA model on the ultimate appearance of the aggregate needs to be examined.

Our computer simulation results were as follows. The distinct effect of limited steps on DLA was the decrease in the efficiency of particles successfully landing on the growing aggregate before they stop. This also quickly leads to anisotropy, leaving only one or two arms continuing to grow if the killing circle technique is used. To model the real track of mobile particles, a Levy flight-type random walk was used [19]. However, the non-restricted launching place condition seemed to compensate for the low efficiency, which results from the limited-step effect to some extent. It turned out that the interior region grew more compactly than that of DLA, in which the interior was screened by the particles arriving previously. However, by adding Voss' concept of the initial distribution of particles to the model, and checking the effect of the atoms in the matrix, we realized that the increase in density in the interior cannot continue after great depletion of the available particles. From this, we concluded that the random matrix not only provided the physical background to randomize the track of mobile particles, but also served as the main source of aggregating particles through atomic collisions.

We observed results similar to those of Voss' model [7]. Figure 4 shows a simulation result with an initial fraction of 0.25. Besides the low efficiency of the limited-step effect, our model seemed also to enhance the depletion around the aggregate compared to Voss' model at the same fraction. While the depletion zone grew along with the aggregation, the structure was observable in the TEM microscope because of the mass contrast.

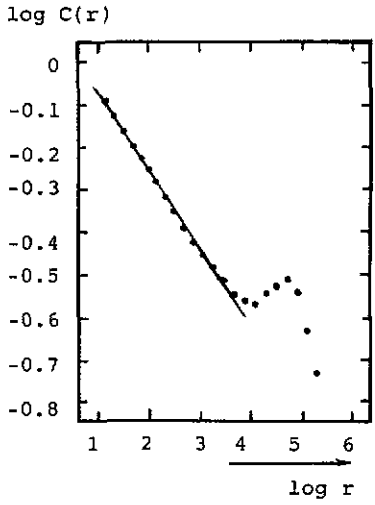

Figure 5. The log–log plot of the correlation function. The unit used for r was pixels. One pixel corresponds to about 0.2 μm. The solid line is a least-squares fit over the range of r up to 50.

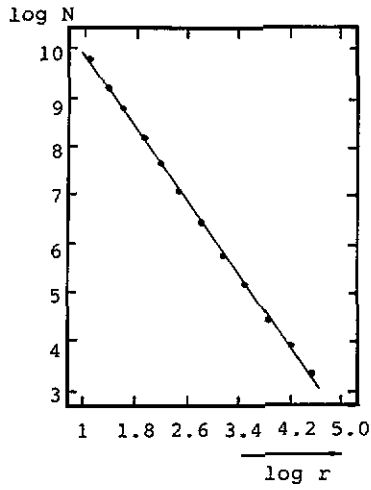

Figure 6. The log–log plot of the number of boxes to cover the structure against the size of box in pixel units. The solid line is a least-squares fit to the data.

To obtain further knowledge of the structure, fractal analysis was conducted by digitizing the pattern in a VAX-IIS computer system with a resolution of 512 × 512 pixels. Various image analysis techniques (such as linear stretching, logarithm stretching, and equivalentizing, etc) were used to decrease background noise and choose the right value of grey-level threshold. The correlation function defined by

$$c(r) = (1/M) \sum \rho(r')\rho(r' + r)$$

showed scaling of

$$c(r) \propto r^{-A}$$

with $A = 0.18 \pm 0.01$ by least-squares fit over the range of r up to about 50 pixels corresponding to 10 μm, as shwon in figure 5. So the fractal dimension $D = 2 - A = 1.82 \pm 0.01$. In the calculation, to eliminate edge effects and ensure equal probability of finding particles in all directions, we chose the centre particles to be those that were the centres of circles whose maximum outer points are within the aggregate. The hump at large r has a large error because fewer points were chosen in the average.

We also calculated the fractal dimension, using Mandelbrot's covering ruler method as demonstrated in the measurement of coastlines [19], by covering the pattern with meshes of different sizes and taking care of coarse graining. We obtained a slightly larger fractal dimension, $D = 1.86 \pm 0.06$, as shown in figure 6. Using the alternative method of sandbox counting, in which pixel numbers in different sizes of box were counted and averaged, we obtained the same results as by using the covering meshes method. The small difference in D obtained with different methods seems intrinsic to statistical fractals: it was also observed in DLA [6] that the fractal dimension obtained using a correlation function was 1.66 but using the mass-gyration method it was 1.70.

The fractal nature, or the dilation symmetry, is better displayed in the enlarged photograph shown in figure 1(*b*). The well-developed small branch impressively

resembles the large one after dilation. The similarity with a DLA structure in side branching and tip splitting can be followed in detail: for example, the angle of side branching, the constant branching or bifurcation after a certain length, etc. An interesting feature of the enlarged photograph was the beauty of the curvature of the bending. One reason proposed for the bending is the natural tendency to explore the available bonding particles in the environment as far as possible, in contrast to the screening in DLA.

Other effects, such as the cluster-diffusion aggregation effect [10] and the real three-dimensionality of the object, have been reported to affect the appearance and the dimension of the structure [20]. But in our estimation such effects are not significant here. For example, in light of the energy of implanting ions, large cluster motion seems to be increasingly unfavourable. The pattern also extended to the order 100 μm while the thickness of the film was only about 100 nm.

From the order of atomic distance (several Ångstroms), we can also obtain an estimation of the number of particles in the aggregate using the scaling property of the fractal—it is of the order of 10^{11}. Including the thickness factor would cause an increase in the number by a factor of 10^2. In spite of the low efficiency caused by the limited step number, the timescale for each mobile particle in the real ion-beam process was of the order of 10^{-13} s. Thus the aggregation was still relatively more efficient than the computer simulation.

In conclusion, DLA-like aggregation processes were observed in ion-implanted thin films. The matrix played two roles: it was the source of active atoms to the aggregation in additon to the implanting particles, and it was the background randomizing the trajectory of the energetic particles. Compared to the DLA model, in the real case, the number of steps each particle undergoes was limited; however, the particles may be launched anywhere, in contrast to their limitation to the outer region of the aggregate in DLA. These factors together change the global appearance and the fractal dimension.

One of the authors (J Wang) wishes to thanks J Cai for constructive discussions about modelling the ion process and for help in experiments, X Y Cheng for help with the simulation program and D Z Che for help in preparations for image analysis. This project is supported by National Natural Science Foundation of China and the International Atomic Energy Agency (contract no 4731/R3/RB).

References

[1] Niemeyer L, Pietronero L and Wiesmann H J 1984 *Phys. Rev. Lett.* **52** 1033
[2] Matsushita M, Sano M, Hayakawa Y, Honjo H and Sawada Y 1984 *Phys. Rev. Lett.* **53** 286
Elam W T, Wolf S A, Sprague J, Gubser D U, Van Vachten D, Barz G L Jr and Meakin P 1985 *Phys. Rev. Lett.* **54** 701
[3] Daccord G, Nittmann J and Stanley H E 1986 *On Growth and Form* ed H E Stanley and N Ostrowsky (Dordrecht: Martinus Nijhoff)
Maløy K J, Feder J and Jøssang T 1985 *Phys. Rev. Lett.* **55** 2688
[4] Radnoczi G, Vicsek T, Sander L M and Grier D 1987 *Phys. Rev. Lett.* **35** 4012
[5] Hurd A J and Schaefer D W 1985 *Phys. Rev. Lett.* **54** 1043
Weits D A and Oliveria M 1984 *Phys. Rev. Lett.* **52** 1433
[6] Witten T A and Sander L M 1981 *Phys. Rev. Lett.* **47** 1400
[7] Voss R F 1984 *Phys. Rev.* B **30** 334
[8] Vicsek T 1984 *Phys. Rev. Lett.* **53** 2281
[9] Botet R and Jullien R 1985 *Phys. Rev. Lett.* **55** 1943

[10] Meakin P 1983 *Phys. Rev. Lett.* **51** 1119
Kolb M, Botet R and Jullien R 1983 *Phys. Rev. Lett.* **51** 1123
[11] Biersack J P and Littmark U 1984 *The Stopping and Range of Ions in Solids* (New York: Pergamon)
[12] Picraux S T and Choyke W J 1982 *Metastable Materials Formation by Ion Implantation* (New York: Elsevier)
[13] Nicolet M-A and Picraux S T 1984 *Ion Mixing and Surface Layer Alloying* (Park Ridge, NJ: Noyes)
[14] Liu B X, Huang L J, Tao K, Shang C H and Li H-D 1987 *Phys. Rev. Lett.* **59** 745
[15] Liu B X, Wang J and Fang Z Z 1991 *J. Phys.: Condens. Matter* **3** 1941
[16] Raig S C and Harding G L 1983 *Surf. Sci.* **124** 591
[17] Pearson W B 1958 *Metal Physics and Physical Metallurgy* (London: Pergamon)
[18] Liu B X, Johnson W L, Nicolet M-A and Lau S S 1983 *Nucl. Instrum. Methods* **209/210** 229
[19] Mandelbrot B B 1983 *The Fractal Geometry of Nature* (San Francisco: Freeman)
[20] Argoul F, Arneodo A, Grasean G and Swinney H L 1988 *Phys. Rev. Lett.* **61** 2558